Electron transport in a disordered semiconductor superlattice

James Leo*
The Blackett Laboratory, Imperial College of Science and Technology, University of London, London SW7 2BZ, United Kingdom
(Received 4 November 1988)

The transport properties of a disordered superlattice in the presence of an applied electric field are studied numerically using the transfer-matrix approach. The effect of disorder on the transmission coefficient as the length of the system and the field is varied is discovered. The existence of Stark ladders in a disordered system is also investigated. The paper concludes by considering transport in a superlattice with a weak magnetic field applied perpendicular to the electric field.

I. INTRODUCTION

Layer-by-layer growth techniques, such as molecular-beam epitaxy (MBE), have made it possible to fabricate structures comprised of alternating layers of two semiconductor materials. By using materials which have different energy-band gaps (for example, GaAs and $Al_{1-x}Ga_xAs$), quantum wells can be formed in the layers of the wider–band-gap material and barriers in the narrower–band-gap material. Because it is possible to select the widths of the wells and barriers by controlling the number of layers that are grown of each material, the bandwidths and band gaps of the resulting device can be predetermined within certain limits. These structures, though, are characterized by very narrow bands which result from the poor coupling between neighboring wells. In some cases this coupling can be so small that the degeneracy between the states in each well is unaffected and consequently no bands are formed.

These multiple–quantum-well structures, termed superlattices, were first introduced by Esaki and Tsu in 1970.[1] Because they are no more than micrometers thick, large electric fields can be produced perpendicular to the layers with use of applied voltages of only a few volts. Experimentally two effects have been found to occur when an electric field is applied across a superlattice. In the first, the field is not dropped linearly across the sample, but only affects a part of it resulting in the formation of a high-field domain. This was discovered by Esaki and Chang[2] and has also been observed by Choi *et al.*[3] and Vuong *et al.*[4] It manifests itself as periodic oscillations in the voltage-current (V-I) characteristics as the high-field domain expands and encompasses more quantum wells. To prevent the formation of a high-field domain, Capasso *et al.*[5] used a structure of the n^+-i-p^+ type, where i is the superlattice. This structure has a built-in bias and so a linear field already exists across it. The field can then be changed by applying a reverse bias and a current produced by illuminating the sample with light.

For a disordered superlattice we will only be considering the second situation in which the field is dropped uniformly across the system. However, in the investigation of a superlattice in a magnetic field both situations will be studied.

The application of an electric field has been shown to result in distortions of the bands resulting in the formation of new eigenstates. It was shown by Zener[6] that the bands of a periodic system slope in the presence of an electric field where the gradient of the bands is given by eF, where e is the electronic charge and F is the electric field strength. This results in the confinement of the electrons within a length W/eF, where W is the band width, now called the Stark length L_S. Wannier[7,8] later introduced the concept of a Stark ladder showing that the energy levels within a sloping band were spaced at intervals of eFa where a is the lattice constant of the periodic system. Stark ladders from different bands can then interact with one another enabling the electrons to Zener tunnel across the band gap.[9–11] In most systems, though, the bands are fairly wide, which results in a Stark length that is longer than the system. However, because a semiconductor superlattice has such narrow bands, the confining effect of the sloping bands is greatly enhanced. Therefore conduction resulting from Zener tunneling between Stark ladders becomes more important. This type of conduction in superlattices has been studied by Movaghar[12] and Leo and MacKinnon.[11]

The growth of superlattices and multiple–quantum-well structures by MBE, however, does not result in perfect interfaces between the barriers and wells. Even in the best devices the control of the growth is only accurate to about two monolayers. Indeed, this has also been shown to be the case in numerical simulations of MBE by Ghaisas and Madhukar[13] and by Clarke and Vvedensky[14] where fluctuations in the growth front are found. There has, however, been some progress in this area with Madhukar *et al.*[15] demonstrating experimentally and Clarke and Vvedensky[14] showing via their numerical work that interruption of the growth process can allow the surface to relax, resulting in smoother interfaces. However, this can then allow impurities that may be present in the growth chamber to deposit onto the surface which can result in further roughening.

The disorder which is induced by these fluctuations in the barrier and well widths can effect the extended Bloch states found in the minibands resulting in the localization of the electrons and consequently a deterioration in the current that can flow. The effect the application of an electric field has on the localizing properties of the disor-

der has been studied to some extent analytically by Leo and Movaghar[16] in the asymptotic limit and numerically by Cota *et al.*[17] and Schwartz and Ting.[18]

In this paper we shall continue on from the approximate analytical work in Ref. 16. We shall use the same recursive transfer-matrix method formulated in that paper to numerically study a finite one-dimensional superlattice in an electric field with different amounts of disorder in the thickness of the barriers and the wells.

II. THE RECURSIVE TRANSFER-MATRIX METHOD

This method was formulated in Ref. 16 where it was used to deal with electric-field-dependent transfer matrices analytically. This allowed an asymptotic form for the transmission coefficient of a one-dimensional disordered chain of square barriers in an electric field to be derived. We shall now briefly review this method.

In the transfer-matrix method, the superlattice under investigation is embedded in an infinite, perfectly ordered system. The wave functions for a single electron in the ordered regions are written

$$\Psi_0 = e^{ik_0 x} + re^{-ik_0 x}, \quad -\infty < x < 1 \tag{1a}$$

$$\Psi_N = te^{ik_N x}, \quad x > N \tag{1b}$$

so that the disordered region extends from $x=1$ to $x=N$. We now connect the plane waves on either side of the superlattice using the transfer matrix $\underline{M}$ to give

$$\begin{bmatrix} t \\ 0 \end{bmatrix} = \underline{M}^N \begin{bmatrix} 1 \\ r \end{bmatrix} . \tag{2}$$

r and t are the reflection and transmission amplitudes, respectively, and $\underline{M}^N$ is the transfer matrix for the whole superlattice and can be written

$$\underline{M}^N = \prod_{i=1}^{N} \underline{m}_i . \tag{3}$$

$\underline{m}_i$ is the transfer matrix for a single barrier and is position dependent in the presence of an electric field. The transmission coefficient for an electron impinging on the superlattice is given by

$$T = \frac{k_N}{k_0} |t|^2 , \tag{4}$$

where k_N and k_0 are the electron's final and initial momentum, respectively. We can rewrite T as

$$T = \frac{k_0}{k_N |(\underline{M}^N)_{11}|^2} , \tag{5}$$

where $(\underline{M}^N)_{11}$ is the (1,1)th element of $\underline{M}^N$. The logarithmic average is now given by

$$\langle \ln T \rangle = \ln(k_N/k_0) - \langle \ln |(\underline{M}^N)_{11}|^2 \rangle . \tag{6}$$

As we only require the first element of $\underline{M}^N$ to find the transmission coefficient, we derive the recursion relation

$$(\underline{M}^N)_{11} = \left[a(n) + \frac{b(n)}{S(n-1)} \right] (\underline{M}^{N-1})_{11} , \tag{7}$$

where

$$S(n-1) = \frac{(\underline{M}^{N-1})_{11}}{(\underline{M}^{N-2})_{11}} \tag{8}$$

and

$$a(n) = m_{11}(n) + \frac{m_{12}(n) m_{22}(n-1)}{m_{12}(n-1)} ,$$

$$b(n) = m_{12}(n) m_{21}(n-1) - \frac{m_{12}(n) m_{22}(n-1) m_{11}(n-1)}{m_{12}(n-1)} . \tag{9}$$

The terms in Eq. (9) relate to the matrix $\underline{m}(n)$ given by

$$\begin{bmatrix} m_{11}(n) & m_{12}(n) \\ m_{21}(n) & m_{22}(n) \end{bmatrix} . \tag{10}$$

$(M^N)_{11}$, and ultimately $\ln T$, can now be found by iterated application of Eq. (7).

III. THE CHAIN OF SQUARE BARRIER POTENTIALS

To model a superlattice we shall use a one-dimensional chain of square barrier potentials and to simulate the type of disorder induced by MBE, we shall randomly vary the widths of the barriers whilst keeping their period constant. We use a square probability distribution ranging from $+D$ to $-D$, where D characterizes the amount of disorder. To include the effect of the electric field, eFx must be subtracted from the potential profile of the barriers. This affects the barriers and wells in two ways. It shifts each unit cell, consisting of a well and barrier, relative to its neighbor by eFa and also alters the shapes of the barriers and wells. We can, however, neglect this second effect and only include the shifting of the wells relative to each other, as it is this effect that introduces the essential physics of the problem. In fact it was shown by Emin and Hart[19] that the alteration in the shapes of the barriers and wells can be incorporated into the periodic potential of the unperturbed system. This has been termed the ladder approximation and been used successfully by many authors (e.g., see Cota *et al.*[17] and Leo and Movaghar[16]).

The matrix elements for $\underline{m}(n)$ within this approximation are

$$M_{11} = \frac{k_1}{4k_3} (\alpha_{21}\alpha_{32} e^{ik_2 b} + \alpha'_{21}\alpha'_{32} e^{-ik_2 b}) \times e^{i(k'_{13} na - k_{13} b/2)} ,$$

$$M_{12} = \frac{-k_1}{4k_3} (\alpha'_{21}\alpha_{32} e^{ik_2 b} + \alpha_{21}\alpha'_{32} e^{-ik_2 b}) \times e^{-i(k_{13} na - k'_{13} b/2)} \tag{11}$$

and $\alpha_{21}=1+k_2/k_1$, $\alpha'_{21}=1-k_2/k_1$, $\alpha_{32}=1+k_3/k_2$, $\alpha'_{32}=1-k_3/k_2$,

$$\begin{aligned} &k_{13}=k_1+k_3, \quad k'_{13}=k_1-k_3 , \\ &k_1^2=[E+F(na-b/2)] , \\ &k_2^2=[E-V_n+F(na-b/2)] , \\ &k_3^2=[E+F(na+b/2)] . \end{aligned} \tag{12}$$

E is the incoming energy and the k's represent the momentum of the electrons in the barrier and wells. Note also that $M_{21}=M_{12}^*$ and $M_{22}=M_{11}^*$.

A further approximation used in Ref. 16 was the random-phase approximation (RPA).[20] It is valid for strong fluctuations in the disorder and reproduces the gross features of the results but it is not sensitive to small effects which might not be producible in experiments anyway. It does this by neglecting multiple reflections from the barriers, which in turn simplifies the calculations. Then the direct product $\underline{m}(n)\otimes\underline{m}^*(n)$, within the RPA, is

$$\underline{m}(n)\otimes\underline{m}^*(n)\approx\begin{bmatrix} |M_{11}|^2 & |M_{12}|^2 \\ |M_{12}|^2 & |M_{11}|^2 \end{bmatrix} . \tag{13}$$

We can now use the recursion relation of Eq. (7) to find $|(\underline{M}^N)_{11}|^2$ instead of $(\underline{M}^N)_{11}$ by substituting the above elements of the matrix into Eq. (9).

IV. TRANSMISSION THROUGH A SYSTEM OF VARYING LENGTH

To find the form for the transmission coefficient as the length of the system is varied, we numerically iterated Eq. (7) for three amounts of disorder and at various electric fields for a system that ranged between 24 barriers and 50 barriers long. To produce two bands the height of the barriers was set at 0.4 eV, the widths of the barriers set at 2.5 nm and the period at 10 nm. The incoming energy of the electron was set at 0.06 eV, which put it approximately in the center of the lower band. The electric field was varied between 0 and 0.05 in renormalized dimensionless units. A field of 0.05 would correspond to about $2x\,10^6$ V m^{-1}. This means that at the greatest field and at the end of the sample the electron has gained enough kinetic energy to give it a total energy that is three times the height of the barrier.

We first studied the zero-disorder case as a kind of reference to compare later results with. Figure 1 displays the results for this case. Each graph in Fig. 1 displays data for a few fields. Figure 1(a) contains the curves for the lowest fields while Fig. 1(c) contains the highest fields. To understand how the electron is affected as it moves through the system in an electric field, we must study each curve on the graphs, following through from one field to the next. Figure 1(a) shows lnT for the zero-field case. As expected, the zero-field curve is hardly changed as the length is increased. Increasing the field results in a linear decrease in ln$T$ corresponding to an exponential decrease in T. However, there is a visible plateau preceding the slope. The last curve on Fig. 1(a), $F=0.008$, and the first curve on Fig. 1(b), $F=0.01$, show that this decrease comes to an end, resulting in the formation of another plateau. But further increases in the field results in another decrease in ln$T$. This can be seen clearly at $F=0.02$. The curve in Fig. 1(c) shows that this decrease, like the previous one, again ends in a plateau.

To understand the origin of these plateaus and the exponential decreases, we calculated the energy the electron had gained from the applied field at the beginning and at the end of the slopes. The start of the first slope in Fig. 1(a) coincides with the electron having gained enough energy to leave the first band. The slope therefore occurs when the electrons is Zener tunneling from one band to the next. The end of this tunneling period coincides with the electron entering the second band. We therefore conclude that the exponential decrease in the transmission coefficient results from the electron traversing the energy gap between the bands and when the electron is moving through a band the logarithm of the transmission coefficient remains constant.

To illustrate this point further, we plotted ln$T$ against length for a system that was 2500 unit cells long at a field of 0.008 (Fig. 2). The plateaus and the slopes are clearly visible and their positions exactly coincide with the edges of the bands. The last decrease in ln$T$ actually occurs above the barriers, which means that there is a forbidden energy region located there. We shall return to this point later.

We shall now consider the effect disorder has on the results obtained for the ordered case. We randomly varied the widths of the barriers by up to 10% ($D=2.5$ Å) of their original width. We, however, kept the period constant so as to not effect the length of the system. As a way of discovering the effect a specific amount of disorder has on the system, we measured the localization length given by the reciprocal of the gradient of a ln$T$-versus-length plot at zero field. In the absence of an electric field the localization is exponential and characterized by a localization length which turns out to be 37 periods long for 10% disorder. We therefore consider this to be the weak-disorder case. The analysis that was carried out in the zero-disorder case is repeated. Figure 3 displays the three graphs showing the results at different fields. The same features that were visible in Fig. 1 for the zero-disorder case clearly still exist. Namely, the plateaus resulting from the electron moving through the bands and the exponential decrease in T characterizing tunneling through the gap. At the very low fields ($F\sim0.001$) the transmission coefficient is not unexpectedly smaller for the disordered case than it was for the ordered one. However, as the field is increased further, there becomes little difference between the transmission coefficient of either the ordered or the disordered superlattice.

Let us now study the stronger-disorder regime. In this case the widths of the barriers were varied by up to 50% ($D=1.25$ nm). Experimentally this would correspond to a very poorly grown MBE sample or a sample consisting of very narrow barrier. From a ln$T$-versus-length plot for the zero-field case the localization length was measured to be ~1.4 periods, which confirms that this is the strong-disorder case. However, when we start increasing

the field, we can see from Fig. 4 that the same plateaus and the same slopes that were present in Figs. 1 and 3 are again present here and that their position with regard to the energy gained by the electron from the field is also the same. It should be noted that an extra decrease in $\ln T$ is visible in both Fig. 3(c) and Fig. 4(c). It occurs when the energy of the electron is above the wells and is caused by a small energy gap that exists there. This is the same gap that can be clearly seen in Fig. 2.

We therefore must conclude that the form for $\ln T$ as the length is varied is only very weakly dependent on the disorder in the presence of an applied electric field. The fact that the positions of the plateaus visible in $\ln T$ are in the same place regardless of the amount of disorder is very interesting but not totally surprising. The disorder that was introduced does not entirely destroy the band structure, but instead reduces the transmissivity of the states within the band and also produces some new states around the edge of it. Namely, all the states within the band become localized with a localization length that depends on the amount of disorder. In three dimensions a mobility edge may exist in the band, separating localized

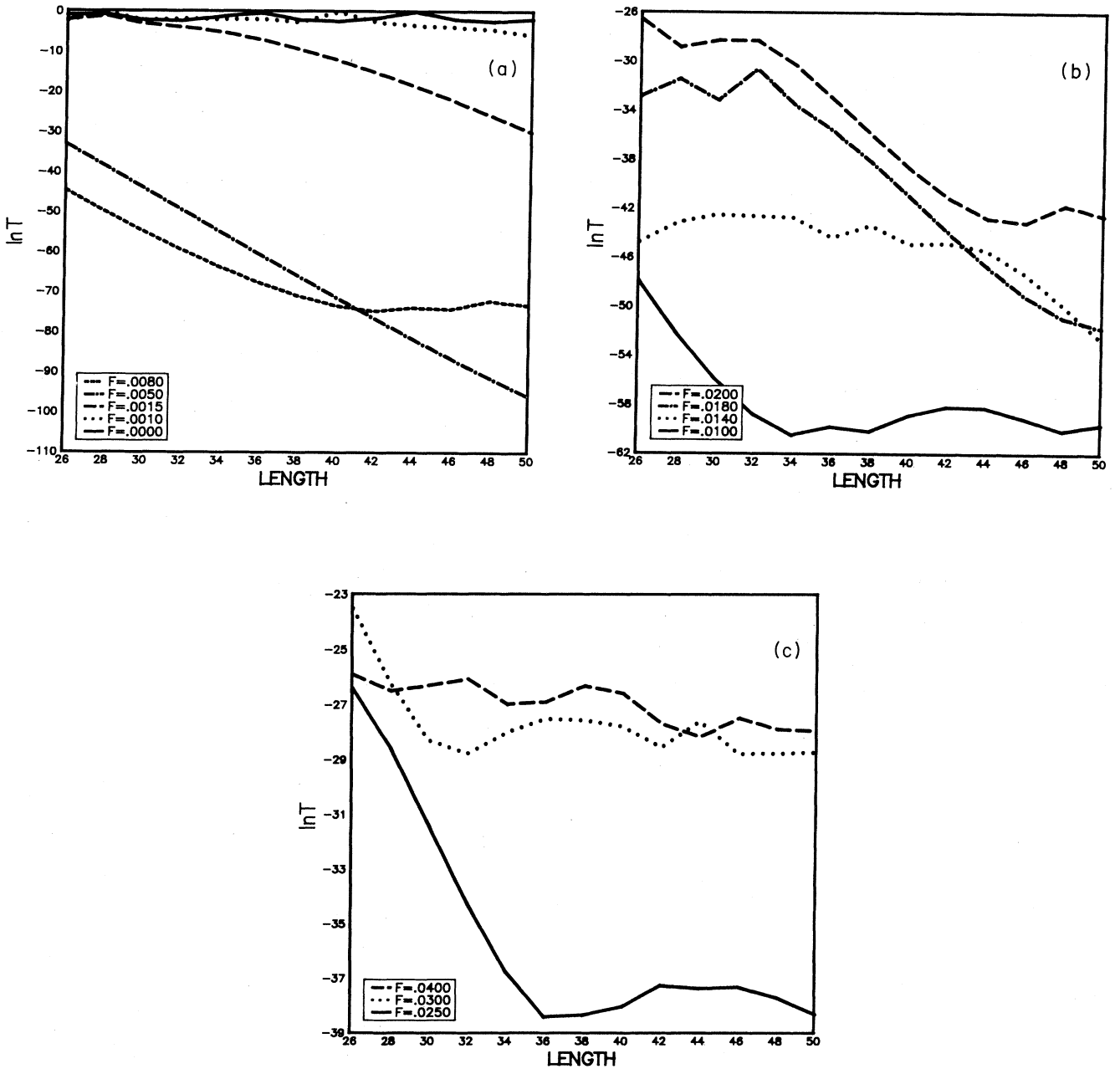

FIG. 1. $\ln T$ as a function of length for a 50-period ordered superlattice plotted at several fields.

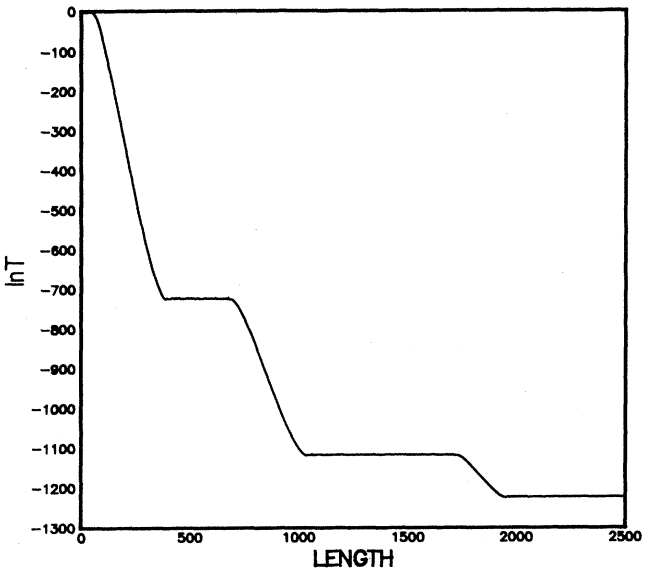

FIG. 2. ln$T$ as a function of length for a 2500-period ordered superlattice at a field of $F=0.008$. Notice the sharp plateaus separated by regions of exponential localization.

states from extended states. When an electric field is applied such that the Stark length becomes less than the length of the system, whether the states are either localized or extended becomes unimportant because the bands are now sloping. This effectively localizes all the states, even in an ordered system. Consequently, the important quantity here is the density of states which, by showing where energy states exist, gives the starting and ending points of the plateaus and slopes in ln$T$. For an averaged system, the width of the density of states is hardly affected by the disorder. Therefore, the positions of the plateaus and slopes, in turn, remain unchanged.

In Ref. 16 the RPA was used to incorporate the disorder into ln$T$ after it had been neglected in the asymptotic limit. It also allowed results to be obtained more simply as $|M_{11}|^2$ could be found from a 2×2 matrix instead of a 4×4 matrix. RPA produces no similar simplification in the numerical calculation as a 2×2 matrix is already being considered. However, it is still used so that a comparison can be made with the exact results.

Figure 5 displays the numerical results using the RPA at different fields. The first thing to notice is that the localization length, obtained from the zero-field curve, is less than 0.34 periods even though a disorder in the barrier of 50% was used. Therefore disorder has a much stronger effect when used within the RPA. This is because multiple reflections that can increase the transmission of the propagating wave are neglected. This also means that no bands are produced and so we do not expect to observe the plateaus in ln$T$. Nevertheless, from Fig. 5 it can be clearly seen that the overall form for ln$T$, especially in the asymptotic limit, is similar to that given in Figs. 1, 3, and 4. We therefore conclude that although RPA enhances the effect of disorder and does not reproduce the effects due to the bands, it can still be used to obtain general forms which are especially applicable in the asymptotic limit.

In similar studies made by Cota *et al.*[17] and Schwartz and Ting[18] of ln$T$ against length in a disordered one-dimensional chain of square barriers, they found jumps in ln$T$. In the paper by Cota *et al.* they attributed this to one of two possible causes, Zener tunneling or the energy of the electron matching a special "delocalization" point in the spectrum. By studying their data one finds that the jumps always occur when the electron has gained a particular amount of energy. On the other hand, Schwartz and Ting believe their jumps are caused by tuning the electron's energy to the energy of a localized state. The jumps are exactly analogous to the slopes in our data. They are caused by the electron Zener tunneling through the band gap and therefore always occur at the same electron energy. The jumps in the data of Cota *et al.* are probably caused by the energy gap that is present far above the tops of the barriers (e.g., the last slope in Fig. 2).

V. TRANSMISSION THROUGH A SYSTEM WITH A VARYING FIELD

A question that may be more pertinent to experiment when the *V-I* characteristics of a device are under consideration is the effect varying the field has on the transmission coefficient. We shall first consider the idealized case of a perfectly ordered superlattice. It has already been mentioned that the application of an electric field results in the formation of a Stark ladder in each band. These ladders of energy states move apart when the field is increased and it was shown in Ref. 11 that at specific values of the field, ladders belonging to different bands come into resonance. We can expect the same kind of effect if we vary the field while the incoming energy of the electron is kept constant. Indeed Fig. 6 shows that as the field is varied, resonances occur in ln$T$. We have set the incoming energy of the electron to be in the gap between the two bands so that the effects due to only one band are observed. The distance between the resonances increases, which points to the possibility that they could be caused by the states in the Stark ladders. This is because the position of the levels in a Stark ladder are given by[21]

$$E_n = eFan + E_0 \ , \tag{14}$$

where n is the Stark label and E_0 is the energy origin of the ladder. Therefore, resonance between the Stark levels and the initial energy E_i occurs when the field is given by

$$F_r = \frac{E_i - E_0}{nea} \ . \tag{15}$$

For all the resonances given in Fig. 6, we plotted F_r against $1/n$ (Fig. 7). Apart from the first section of the graph, the points lie on a very good straight line. The deviation from the straight line at low fields is caused by boundary conditions. At the edges of the sample the distance between Stark levels is not eFa but is much larger. This, coupled with the fact that the resonances at low

fields are caused by the electron using these edge states as paths of conductance, results in the curve in Fig. 7.

We repeated the above calculation but this time we moved the initial energy of the electron so that it lay below both bands. In Fig. 8 the consequences of having to traverse both Stark ladders can now be observed with two sets of resonances present and superimposed upon each other. The resonances resulting from the Stark ladder in the higher band start at a much higher field (~ 0.008) and are initially visible as much weaker resonances.

The introduction of disorder into the system must clearly affect the Stark resonances. To understand how, we shall return to the derivation of a Stark ladder in an ordered system. Schrödinger's equation for a periodic system in the presence of an electric field is

$$\left[\frac{p^2}{2m^*}+V(x)-eFx\right]\Psi(x)=E\Psi(x)\ . \tag{16}$$

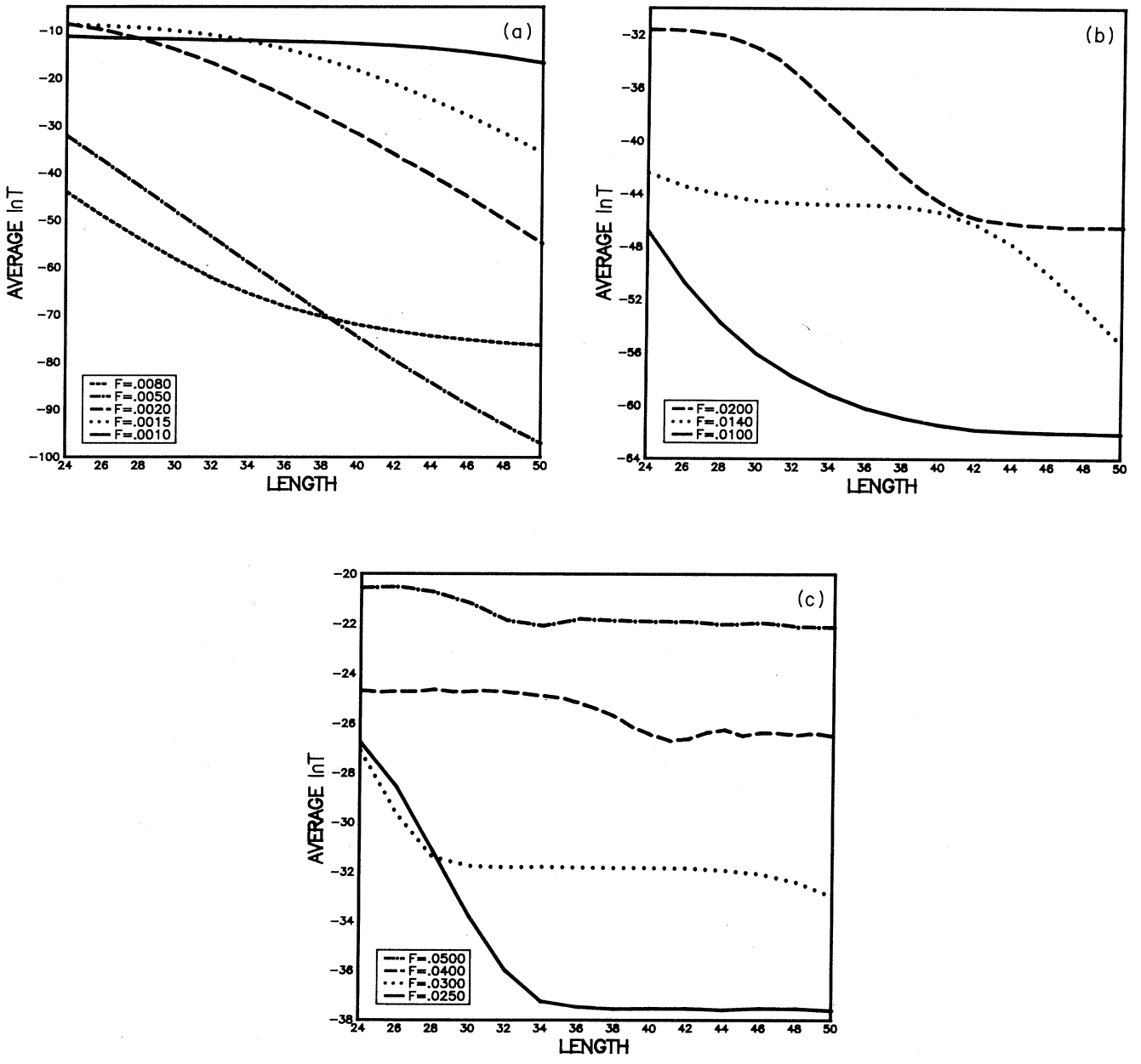

FIG. 3. The arithmetic average of $\ln T$ as a function of length for a 50-period weakly disordered superlattice plotted at several fields.

If we now translate (16) by a lattice constant a, we get

$$\left[\frac{p^2}{2m^*}+V(x)-eFx\right]\Psi(x+a)=(E+eFa)\Psi(x+a)\ . \tag{17}$$

Therefore, if an energy level exists at E, then another exists at $E+eFa$. We can now translate Eq. (16) by any number of lattice constants to give a ladder of energy levels with a separation of eFa between the levels [Eq. (14)]. However, with disorder in the system $V(x+a)$ no longer equals $V(x)$. Therefore, translating (16) by a now gives

$$\left[\frac{p^2}{2m^*}+V(x)+V'(x)-eFx\right]\Psi(x+a) =(E+eFa)\Psi(x+a)\ , \tag{18}$$

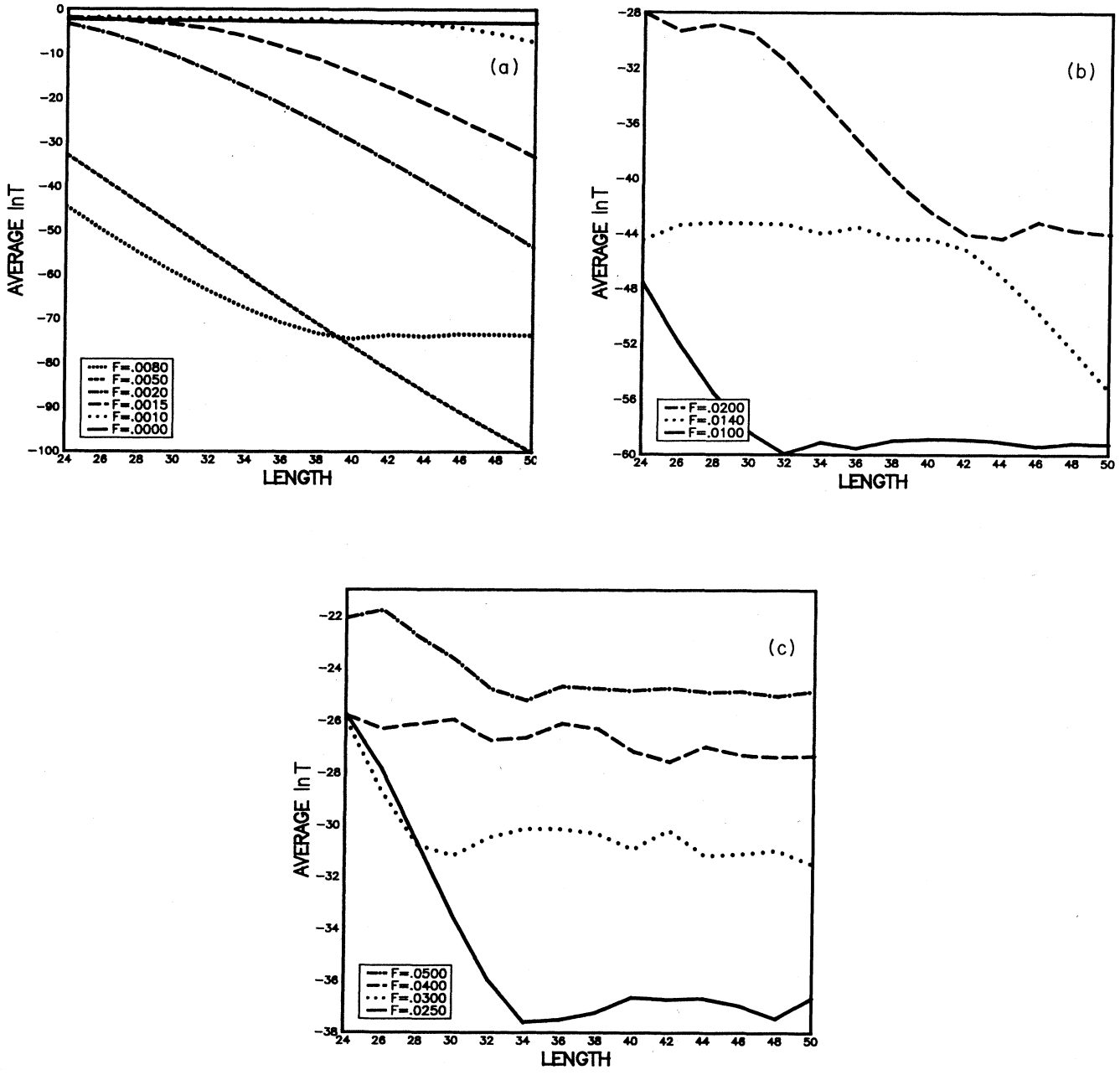

FIG. 4. The arithmetic average of $\ln T$ as a function of length for a 50-period strongly disordered superlattice plotted at several fields.

where V' is the extra potential caused by the disorder. If we write

$$V'(x)\Psi(x+a)=\varepsilon\Psi(x+a)\ , \tag{19}$$

we obtain an addition of a random energy ε to $E+eFa$. Nonetheless, the important result is that the Stark ladder still exists, albeit somewhat modified, even in the presence of disorder.

To confirm this we plotted $\ln T$ against field for two samples, one with strong disorder (50%) and one with weak disorder (10%). The electron was injected between the two bands so that the effect of just one Stark ladder is observed. No averaging was carried out on these samples so that the numerical results we obtained would give an indication of the type of output that might be observed experimentally when every sample is unique and not an average.

Figure 9 shows that the results in the weak-disorder limit are not very different from the results in the ordered case given by Fig. 6. The difference is now that the posi-

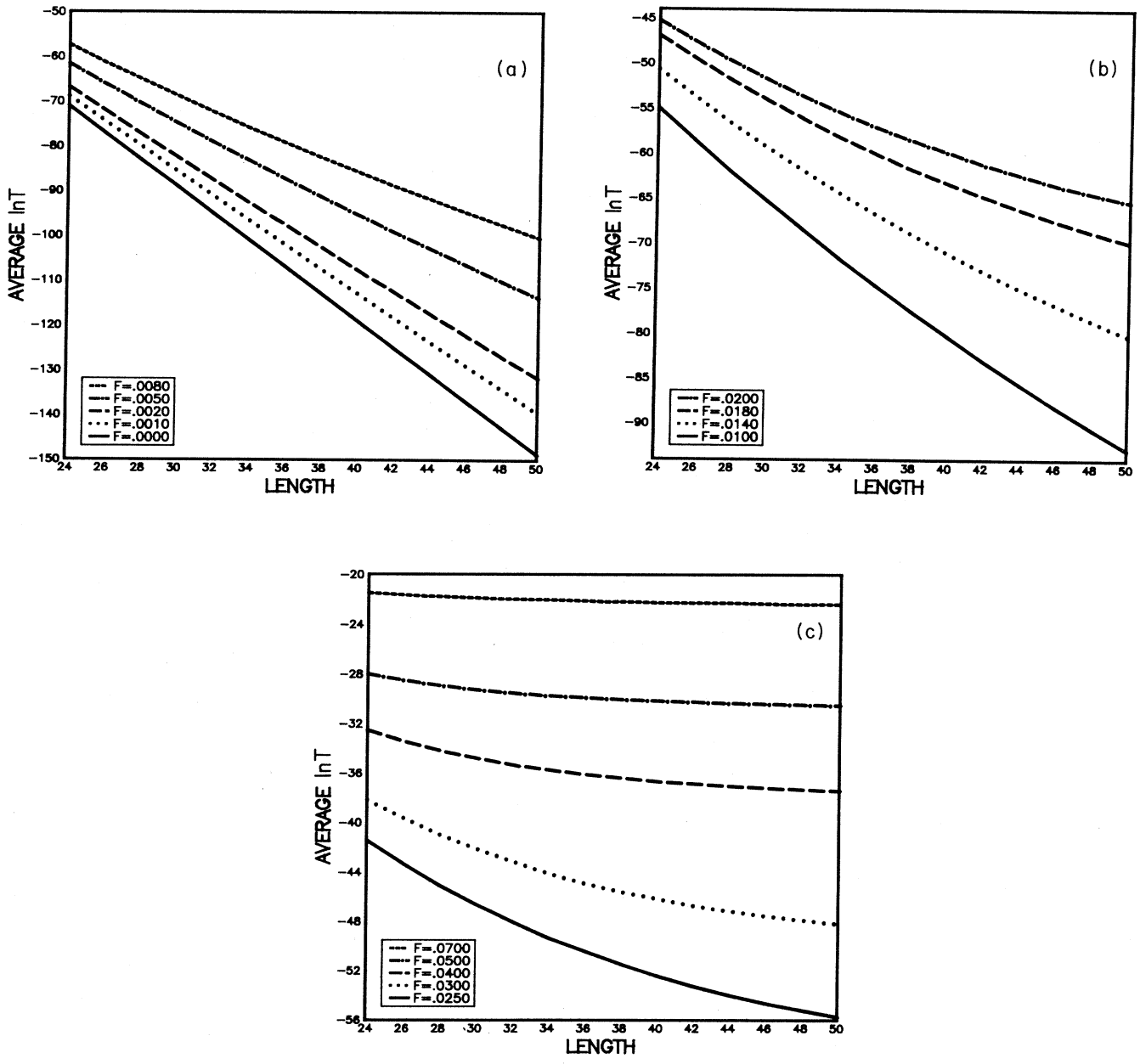

FIG. 5. The arithmetic average of $\ln T$ as a function of length for a 50-period strongly disordered superlattice plotted at several fields within the RPA.

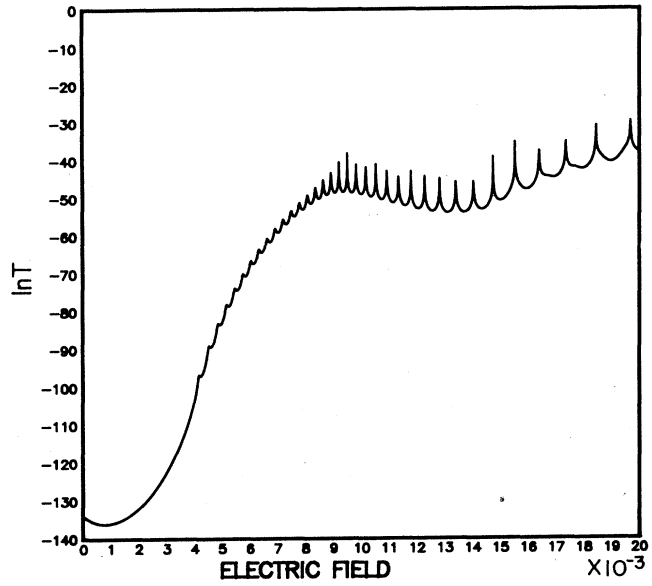

FIG. 6. ln$T$ vs electric field for a ordered superlattice. Only tunneling through one band is being considered.

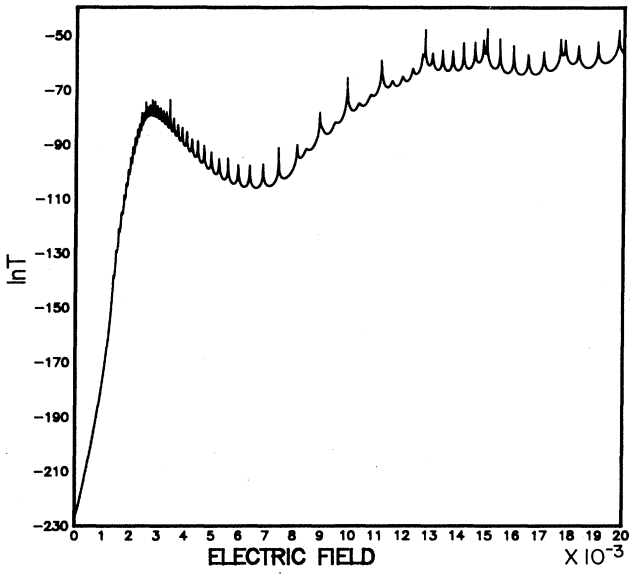

FIG. 8. ln$T$ vs electric field for a ordered superlattice. Tunneling through two bands is now being considered.

tions of the resonances are not well defined but can fluctuate by an amount given by the amount of disorder D. Consequently, as expected, the positions of the resonances in the strong-disorder case (Fig. 10) are even more random. If these results were averaged to simulate thermal or similar effects, then of course these rather elegant resonances would not exist. We also studied ln$T$ within RPA (Fig. 11). Application of the field results in a very rapid initial rise in ln$T$ which seems to be exponential in T. However, as the field is increased further ln$T$ starts to tail off, tending to a constant value in the asymptotic limit. Again, by comparing Fig. 11 with Fig. 6, we can see that RPA reproduces the course features of the results.

VI. CROSSED ELECTRIC AND MAGNETIC FIELDS

The transfer-matrix method used in this paper can be very simply adapted to study how the flow of electrons through the superlattice is affected by applying a weak magnetic field perpendicular to the electric field. This type of situation has not been studied to any appreciable

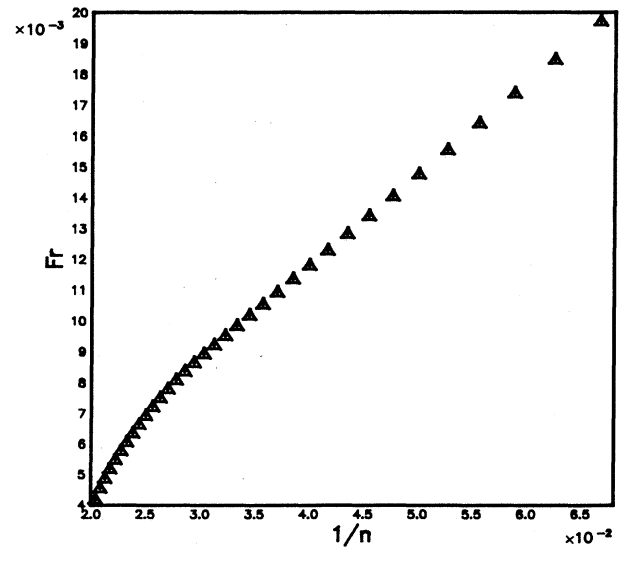

FIG. 7. A plot of the field at which the resonances in Fig. 6 occur vs the reciprocal of the indices characterizing the Stark states.

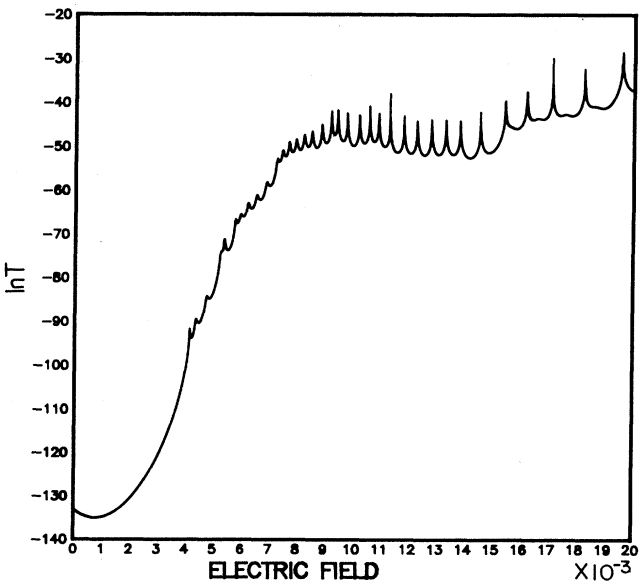

FIG. 9. ln$T$ vs electric field for a weakly disordered superlattice.

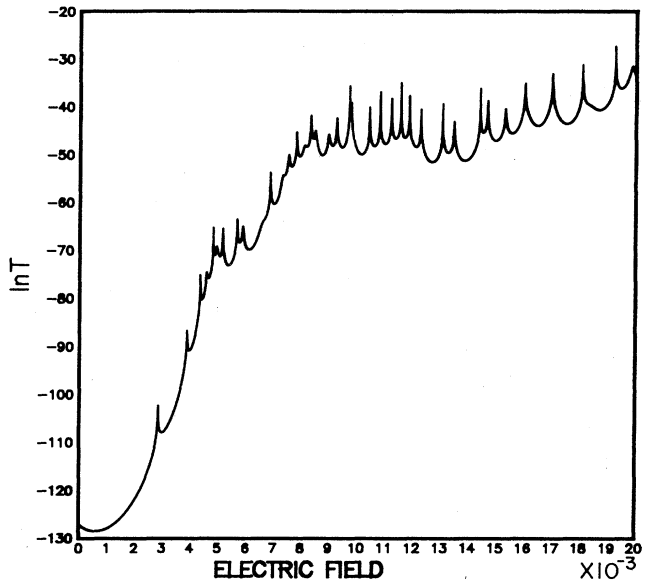

FIG. 10. ln$T$ vs electric field for a strongly disordered superlattice.

degree or extent. Much work has instead been channeled into the situation where the magnetic field is applied parallel to the quantum-well interfaces (i.e., perpendicular to the two-dimensional electron gas in the wells). This has provided some very interesting physics (i.e., Klitzing *et al.*[22]).

The effect a magnetic field has on a GaAs/$Al_{1-x}Ga_xAs$ superlattice structure has been studied experimentally by Davis *et al.*[23] Their superlattice, however, was not uniform but consisted of two super lattices coupled together via a thick barrier. Consequently

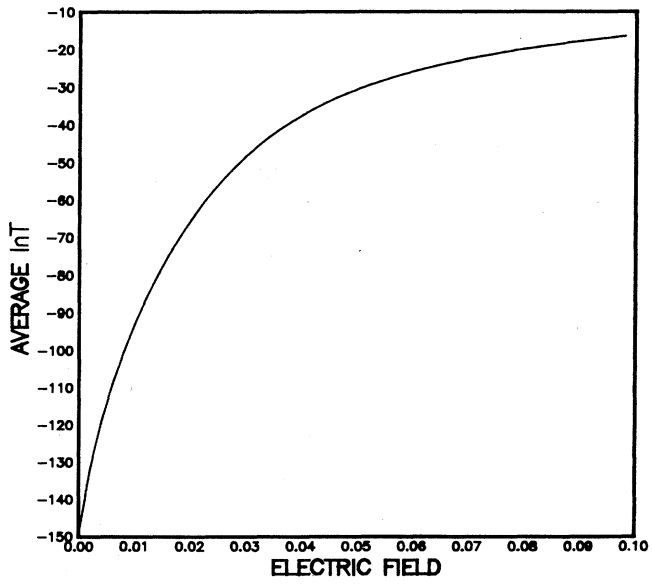

FIG. 11. The arithmetic average of ln$T$ plotted against electric field for a disordered superlattice within the RPA.

most of the bias was dropped across this one barrier, misaligning the superlattice minibands on either side. Apart from this effect, the bands themselves were fairly unaffected by the electric field (i.e., they did not slope). The *V-I* characteristics of this structure at zero magnetic field were found by Davis to contain a region of negative differential resistance (NDR) resulting from the misaligning of the minibands. The application of the magnetic field perpendicular to the electric field was observed to have two effects on the NDR. At low magnetic fields it moved to higher biases, but as the magnetic field was increased to over 10 T the NDR completely disappeared. Similar work has been carried out by Eaves *et al.*,[24] Hickmott,[25] and by Lebens *et al.*[26] who studied tunneling through a single-barrier system with crossed electric and magnetic fields.

Let us first consider the full three-dimensional superlattice where the superlattice period is in the x direction, and the electrons are plane waves in the other two dimensions. The application of magnetic field B in the z direction results in the following Hamiltonian in the Landau gauge:

$$H=[p_x^2+p_z^2+(p_y-eBx)^2]\frac{1}{2m^*}-eFx+V(x)\ . \tag{20}$$

If we now make the ansatz that the solution to Schrödinger's equation with the above Hamiltonian has plane waves in the y and z directions, we can write

$$\left[\frac{p_x^2}{2m^*}-eFx+V(x)+\frac{e^2B^2x^2}{2m^*}-\frac{eB}{m^*}xp_y\right]\Psi_\nu(x) =E_\nu\Psi_\nu(x)\ , \tag{21}$$

where ν labels the Landau levels. Therefore the application of an electric field results in two extra terms in the Hamiltonian, a quadratic "oscillator" term and a linear term. This linear term can be absorbed into the electric field so that

$$eF'\rightarrow eF+\frac{eB}{m^*}p_y\ . \tag{22}$$

If we now make the approximation that B is sufficiently weak such that the cyclotron radius a_0, where $a_0^2=\hbar/eB$, is much greater that the width of the barrier layers b, then the effect B has on the matrix elements between neighboring wells can be neglected. Therefore, the only effect Eq. (21) has is to shift the energy of one well with respect to its neighbor by

$$-eFb+\frac{e^2B^2}{2m^*}b^2-\frac{eBb}{m^*}p_y\ . \tag{23}$$

Note that now the energy the electrons gain by crossing the barrier between the two wells is no longer just a function of position but also a function of its transverse momentum p_y.

The above formulation can now be incorporated into the transfer-matrix method by simply modifying the k momenta in each well and barrier section given in Eq.

(12) by the amount given in Eq. (23). The linear term now exaggerates the effect of the electric field term to further increase the kinetic energy of the electron as it moves through the system. However, there is also a positive quadratic term which reduces the energy of the electron. In the limit of a weak magnetic field we expect that over several quantum wells the linear energy terms will dominate. However, the quadratic positive term will eventually take over, causing the localization of electrons into cyclotron orbits. Because of the importance of the perpendicular momentum p_y in this type of calculation, electrons with p_y ranging from zero to the Fermi energy will be allowed to contribute to the current.

Two types of structures were investigated using this technique. Both were superlattices consisting of ten barrier well periods, but the electric field affected them both in different ways. In the first sample, all the field was dropped across the last barrier. This could therefore represent a double-barrier structure or a system similar to Davis's. Figure 12 shows the results obtained for four magnetic fields, 0, 1, 2, and 3 T. The period of the structure corresponded to about 10 nm and an electric field of one unit was equivalent to about 5×10^3 V/cm.

At zero magnetic field the peak caused by the alignment of the bound state in the last well and the incident energy of the electron is clearly visible at $F=15$. As B is increased two effects are observed in complete agreement with that found by Davis. First the peak becomes much broader as the bound state becomes resonant with electrons at different p_y. This obviously strongly effects the NDR. Then as the magnetic field is increased further up to 2 T, the peak moves to higher biases and becomes even more broad as the bound state becomes resonant with even more electrons, all with different transverse momentum. Finally an increase of B to 3 T was found to further exaggerate these features.

The plateau formed on the now-broadened peak is caused by the sum over the transverse momentum p_y in the following way. An electron with a particular p_y will form a particular V-I curve. Studying an electron with a different p_y is equivalent to studying an electron with the previous p_y but at a different electric field [this can be seen from Eq. (22)]. Therefore the electron with this new p_y produces the same shape V-I curve as the electron with the previous p_y but it is now shifted along the electric field axis. Consequently, peaks in the V-I curves are formed into plateaus.

In the second structure the field was allowed to drop uniformly across the whole system. This would result in the formation of the now familiar Stark states and Stark ladder, although now, because the system is so short, these states may be strongly affected by the boundaries. Figure 13 shows the results obtained for zero magnetic field and for a field of 1 T. At $B=0$ the same Stark resonances that were observed in Fig. 6 are again visible. The application of the magnetic field causes a broadening out of the resonances to such an extent that the ones at low biases almost disappear completely. However, the resonances at the higher biases turn into groups of seven miniresonances. These exist because the magnetic field makes it possible for electrons with different p_y to tunnel resonantly via other Stark states. In a real system these resonances would be smeared out by scattering.

An effect observable in Fig. 13 and which is contrary to the features in Fig. 12 and the observations made by Davis is that the broadened NDR has moved to lower biases instead of higher biases, resulting in a negative

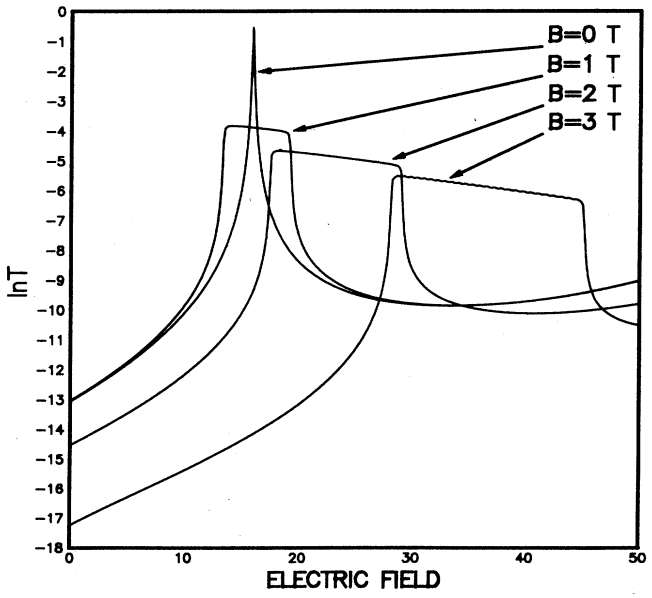

FIG. 12. ln$T$ vs electric field for a ten-period superlattice with all the electric field dropped across the last barrier. The resonance is displayed for four magnetic fields.

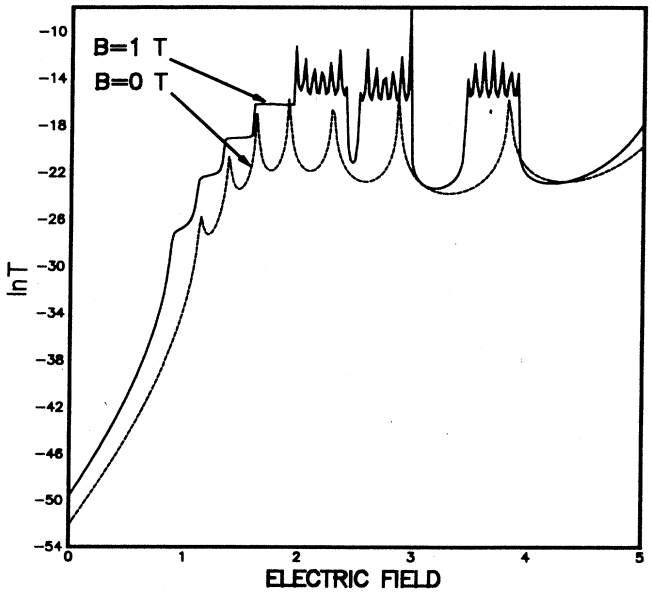

FIG. 13. ln$T$ vs electric field for a ten-period superlattice with the electric field now dropped uniformly across the whole structure. The Zener resonances are shown for two values of the magnetic field.

magnetoresistance. This results from the fact that the linear terms in (23) are dominating over the quadratic term. In Fig. 12 the opposite was true.

VII. CONCLUSION

We have studied the effect disorder has on transport in a semiconductor superlattice in an electric field. By investigating the dependence of $\ln T$ on the length of the system, we have discovered that it is not the amount of disorder which is important if the electric field is large enough such that the Stark length is less than the system size. What effects the transport properties much more is the number of bands and their widths. This is because $\ln T$ has two functional dependences on position depending on whether the electron's energy puts it in one of the bands or one of the gaps when it has reached the end of the system.

To relate the numerical work more closely to experiment, in particular the voltage-current characteristics, the system size was kept constant and the electric field was varied. In the absence of disorder, aperiodic resonances were discovered in $\ln T$ as the field was increased. These were found to result from the Stark levels in the bands lining up with the electron's initial energy to produce an enhanced conductance path. After introducing disorder into the system, we found that it did not totally destroy the Stark ladder structure but merely modified the positions of the levels within the ladders by a random amount. This consequently showed up as resonances in $\ln T$ with slightly random positions. We therefore note the possibility of using the Stark resonances that might exist in the current as an indicator of the amount of disorder in a particular sample.

We also found that the application of a weak magnetic field perpendicular to the electric field could be incorporated very simply into the formalism. Although the technique was very approximate, the initial results we obtained reproduced the essential features observed experimentally. The limiting factor in the calculations was the cyclotron radius which can become comparable to the well-barrier period at fields of 3 T or less.

ACKNOWLEDGMENTS

I would like to thank the United Kingdom Science and Engineering Research Council and GEC Research Limited (Wembley, United Kingdom) for financial support and Dr. A. MacKinnon and Dr. B. Movaghar for useful discussions.

---

*Present address: Max-Planck-Institut für Festkörperforschung, Heisenbergstrasse 1, Postfach 800665, D-7000 Stuttgart 80, Federal Republic of Germany.

[1]L. Esaki and R. Tsu, IBM J. Res. Dev. **14**, 61 (1970).
[2]L. Esaki and L. Chang, Phys. Rev. Lett. **2**, 185 (1974).
[3]K. K. Choi, B. F. Levine, R. J. Malik, J. Walker, and C. G. Bethea, Phys. Rev. B **35**, 4172 (1987).
[4]T. H. H. Vuong, D. C. Tsui, and W. T. Tsang, Appl. Phys. Lett. **52**, 981 (1988).
[5]F. Capasso, K. Mohammed, and A. Y. Cho, Appl. Phys. Lett. **48**, 478 (1986).
[6]C. Zener, Proc. R. Soc. London, Ser. A **145**, 523 (1934).
[7]G. H. Wannier, *Elements of Solid State Theory* (Cambridge University Press, London, 1954), pp. 190–193.
[8]G. H. Wannier, Phys. Rev. 117, 432 (1960).
[9]H. Fukuyama, R. A. Bari, and H. C. Fogedby, Phys. Rev. B **8**, 5579 (1973).
[10]J. E. Avron, Ann. Phys. (N.Y.) **143**, 33 (1982).
[11]J. Leo and A. MacKinnon, J. Phys. C (to be published).
[12]B. Movaghar, Semicond. Sci. Technol. **2**, 185 (1987).
[13]S. V. Ghaisas and A. Madhukar, J. Vac. Sci. Technol. B **3**, 540 (1985).
[14]S. Clarke and D. D. Vvedensky, Appl. Phys. Lett. **51**, 340 (1987).
[15]A. Madhukar, T. C. Lee, M. Y. Yen, P. Chen, J. Y. Kim, S. V. Ghaisas, and P. G. Newman, Appl. Phys. Lett. **46**, 1148 (1985).
[16]J. Leo and B. Movaghar, Phys. Rev. B **38**, 8061 (1988).
[17]E. Cota, J. V. José, and M. Ya. Azbel, Phys. Rev. B **32**, 6157 (1985).
[18]C. Schwartz and C. S. Ting, Phys. Rev. B **36**, 7169 (1987).
[19]D. Emin and C. F. Hart, Phys. Rev. B **36**, 7353 (1987).
[20]D. J. Thouless, in *Physics of One Dimension,* Vol. 23 of *Springer Series on Solid States,* edited by J. Bernasconi and T. Schneider (Springer, Berlin, 1981).
[21]M. Saitoh, J. Phys. C **5**, 914 (1972).
[22]K. von Klitzing, G. Dorda, and M. Pepper, Phys. Rev. Lett. **45**, 494 (1980).
[23]R. A. Davis, D. J. Newson, T. G. Powell, M. J. Kelly, and H. W. Myrons, Semicond. Sci. Technol. **2**, 61 (1987).
[24]L. Eaves, K. W. H. Stevens, and F. W. Sheard, in *The Physics and Fabrication of Microstructures and Microdevies,* edited by M. J. Kelly and C. Weisbuch (Springer-Verlag, Berlin, 1986), p. 343.
[25]T. W. Hickmott, Solid State Commun. **63**, 371 (1987).
[26]J. A. Lebens, R. H. Silsbee, and S. L. Wright, Phys. Rev. B **37**, 10 308 (1988).